Transport properties of arrays of elliptical cylinders

N. A. Nicorovici and R. C. McPhedran
Department of Theoretical Physics, School of Physics, University of Sydney, New South Wales 2006, Australia
(Received 20 March 1996)

We apply the Rayleigh method to derive a formulation yielding the effective dielectric tensor of a periodic composite consisting of an array of elliptical cylinders placed in a matrix of unit dielectric constant. We consider three types of composites having this structure: dilute noncritical, dilute critical, and concentrated composites. For dilute noncritical composites we comment on our result in relation to the competing forms of the Maxwell-Garnett formula, which have been proposed previously. We also discuss the case of dilute critical and concentrated composites of solid elliptical inclusions, and comment on geometrical constraints on the validity of the Rayleigh equations. [S1063-651X(96)00908-7]

PACS number(s): 03.50.De, 41.20.Cv, 78.20.Bh, 78.20.Ci

I. INTRODUCTION

Analysis concerning the transport properties of inhomogeneous systems is of fundamental theoretical interest, but also plays an important role in optimal designs of industrial products. For example, many modern structural materials depend on the use of composite materials. It is also possible to produce columnar thin films which are highly conducting. In particular, thin films containing metal and voids in an oblique columnar structure exhibit angular dependent optical properties [1,2]. By forming the columns at an angle and coating them with metal, highly conducting elliptical cylinders can be produced. Such a capacitive grid can manifest strong angular selectivity as a result of the basic asymmetry of the component ellipses. Materials with such characteristics may have uses in filters, windows in residential and commercial buildings, and car windscreens [1–3].

Here, using the terminology for the calculation of the dielectric constant, we analyze the transport properties of a two-dimensional two-phase composite material consisting of a rectangular array of elliptical cylinders placed in a matrix of unit dielectric constant (with the principal axes of the ellipses coinciding with the periodicity axes of the array). To obtain the effective dielectric constant of the array we use the method devised by Lord Rayleigh [4], for rectangular arrays of circular cylinders. Rayleigh's method has been extended to include an arbitrary number of terms and applied in studies of arrays of cylinders [5–7], arrays of coated cylinders [8–10], lattices of spheres [11,12], and lattices of coated spheres [10]. This method has also been used in problems of elastostatics [13,14]. Note that the same formalism and the results are immediately applicable to many other transport coefficients including those listed by Batchelor [15]; e.g., thermal conductivity, electrical conductivity, magnetic permeability, mobility, permeability of a porous medium, modulus of torsion in a cylindrical geometry, and effective mass in a bubbly flow.

The technique used in this paper represents an extension of Rayleigh's method to noncircular boundaries of the inclusions. In this paper we apply the Rayleigh method to such boundaries. Generally, Rayleigh's method involves the calculation of certain static lattice sums, which contain information about the geometry of the array. We show that, imposing certain geometrical constraints on the aspect ratios of the unit cell and inclusions, only the lattice sums in polar coordinates are needed. With the exception of the lattice sum σ_2, which is conditionally convergent, all the other polar lattice sums are absolutely convergent and can be evaluated with arbitrary high accuracy [4,7,14,16,17]. The lattice sum σ_2 is related with the depolarization field and methods for evaluation have been devised [4,7,14,16,17].

Structures involving rectangular arrays are intrinsically of interest since they permit inclusions to come close to touching, even when the area fraction of the inclusions is small (e.g., if inclusions are in close proximity along the y axis but well spaced along the x axis). It is thus necessary to distinguish the concepts of critical composites, where inclusions come close to each other, from dilute composites, where the area fraction of the inclusions is small. We study all three cases: dilute noncritical composites, dilute critical composites, and concentrated critical composites.

For dilute noncritical composites, structured as rectangular arrays of elliptical cylinders, we derive a Maxwell-Garnett type formula and comment on our result in relation to other formulas of a Maxwell-Garnett type, which have been proposed previously. In this way, we solve a controversy concerning the correct form of this relationship for composites with elliptical inclusions [18–20]. For dilute critical composites, we exhibit a correction to the Maxwell-Garnett formula which renders it useful even in the region where the array dielectric constant is large. For concentrated systems, we establish the geometrical constraints on the validity of our method.

II. RAYLEIGH'S IDENTITY FOR ELLIPTICAL CYLINDERS

We consider a rectangular array of infinitely long elliptical cylinders embedded into a host medium of dielectric constant ε_0. The dielectric constant of the cylinders (ε) is specified as its ratio to the dielectric constant of the host medium, so that we will use $\varepsilon_0 = 1$. The cross sections of the cylinders are ellipses with the foci distance $2c$. The semiaxes of the cross section of the cylinders are denoted by r_1 and r_2 (Fig. 1). Note that the discussion which follows implicitly assumes $r_1 \geqslant r_2$: the modifications required to deal with $r_2 > r_1$ are

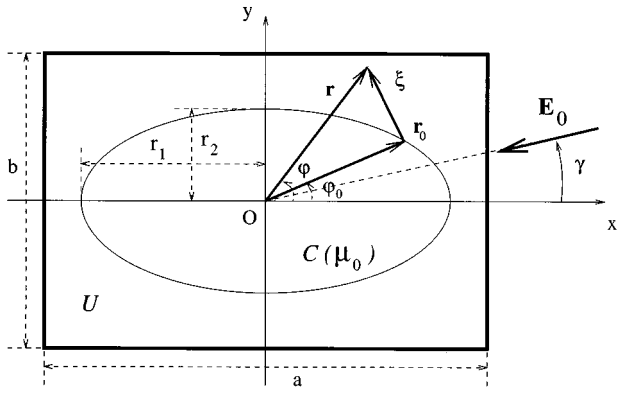

FIG. 1. The unit cell for a rectangular array of elliptical cylinders. The semiaxes of the ellipse are r_1 and r_2. In elliptical coordinates the ellipse is defined by μ_0 through the relations $r_1=c\cosh\mu_0$, $r_2=c\sinh\mu_0$. We also show the incident field $\mathbf{E}_0$.

obvious. The cylinders in the array are subject to a uniform electric field $\mathbf{E}_0$, exterior to the region occupied by cylinders, which makes an angle γ with the x axis. The problem we have to solve is to find the effective dielectric tensor of the array ($\tilde{\varepsilon}^*$) by means of Rayleigh's method [4].

The shape of the cross section of the cylinders defines the most appropriate system of coordinates for the solution of Laplace's equation. Thus inside the unit cell centered at the origin (Fig. 1), in elliptical coordinates [21,22]

$$x=c\cosh\mu\cos\theta, \tag{1}$$

$$y=c\sinh\mu\sin\theta, \tag{2}$$

the cross section of the cylinder is defined by $\mu=\mu_0$. The ellipse (C) divides the unit cell into two regions, where the expansions of the potential are (see Appendix A)

$$V_e(\mu,\theta)=2A_0^e+B_0^e+\sum_{n=1}^{\infty}\left\{\left[2A_n^e\left(\frac{c}{2}\right)^n\cosh(n\mu)+B_n^e\left(\frac{2}{c}\right)^n e^{-n\mu}\right]\cos(n\theta)+\left[2A_n^o\left(\frac{c}{2}\right)^n\sinh(n\mu)+B_n^o\left(\frac{2}{c}\right)^n e^{-n\mu}\right]\sin(n\theta)\right\}, \tag{3}$$

for $\mu\geqslant\mu_0$, and

$$V_i(\mu,\theta)=2C_0^e+\sum_{n=1}^{\infty}\left[2C_n^e\left(\frac{c}{2}\right)^n\cosh(n\mu)\cos(n\theta)+2C_n^o\left(\frac{c}{2}\right)^n\sinh(n\mu)\sin(n\theta)\right], \tag{4}$$

for $\mu\leqslant\mu_0$. We use the labels e and o to emphasize that the corresponding coefficients are related with an even or an odd function of θ. Also, due to the symmetry properties of the potential with respect to the reflections $x\to -x$ and $y\to -y$, the index n in (3) and (4) has to be odd.

The Rayleigh identity for our problem follows from Green's theorem, applied to the general solution of Laplace's equation (3) and Green's function (see Appendix B), inside the unit cell, in the domain between the ellipse $C(\mu_0)$ and the boundary of the unit cell (∂U)

$$\int_{U\setminus C}[G(\mu,\theta;\mu',\theta')\nabla^2V_e(\mu',\theta')-V_e(\mu',\theta')\nabla^2G(\mu,\theta;\mu',\theta')]dA'=\oint_{(\partial U)\cup(\partial C)}\left[G(\mu,\theta;\mu',\theta')\frac{\partial V_e(\mu',\theta')}{\partial n'}-V_e(\mu',\theta')\frac{\partial G(\mu,\theta;\mu',\theta')}{\partial n'}\right]d\ell'. \tag{5}$$

By substituting in (5) the expansion (B18) for Green's function, and (3) for V_e we obtain the Rayleigh identity for a rectangular array of elliptical cylinders (see Appendix C)

$$\sum_{j\ \text{odd}}2\left(\frac{c}{2}\right)^j[A_j^e\cosh(j\mu)\cos(j\theta)+A_j^o\sinh(j\mu)\sin(j\theta)]=V_0(\mu,\theta)-\sum_{m\ \text{odd}}\sum_{n=m}^{\infty}\sum_{\ell=0}^{2n-m}\left\{\left(\frac{c}{2}\right)^{2n-m}\binom{2n}{\ell+m}\times\binom{2n}{\ell}\frac{m}{2n}\sigma_{2n}[B_m^e\cos(2\ell+m-2n)\theta-B_m^o\sin(2\ell+m-2n)\theta]e^{(2\ell+m-2n)\mu}\right\}, \tag{6}$$

where V_0 is the potential for the applied field [21]

$$V_0(\mu,\theta)=E_0c(\cosh\mu\cos\theta\cos\gamma+\sinh\mu\sin\theta\sin\gamma), \tag{7}$$

and σ_{2n} are static lattice sums [see (B12)]. From (6), using the orthogonality of the trigonometric functions, we obtain two linear systems

$$A_{2j-1}^e+\sum_{m=1}^{\infty}\Lambda_{2j-1,2m-1}(c)B_{2m-1}^e=E_0\cos\gamma\,\delta_{j,1}, \tag{8}$$

$$A_{2j-1}^o-\sum_{m=1}^{\infty}\Lambda_{2j-1,2m-1}(c)B_{2m-1}^o=E_0\sin\gamma\,\delta_{j,1}, \tag{9}$$

for $j=1,2,3,\ldots$. Here,

$$\Lambda_{2j-1,2m-1}(c)=\binom{2j+2m-3}{2j-1}\sigma_{2j+2m-2}+\lambda_{2j-1,2m-1}(c), \tag{10}$$

with

$$\lambda_{2j-1,2m-1}(c)=\sum_{n=j+m}^{\infty}\binom{2n}{n+j+m-1}\binom{2n}{n+j-m}\times\left(\frac{c}{2}\right)^{2n-2m-2j+2}\frac{2m-1}{2n}\sigma_{2n}. \tag{11}$$

In the case of a rectangular array with the sides a and b, and $a>b$, the static lattice sums σ_{2n} can be written in the form

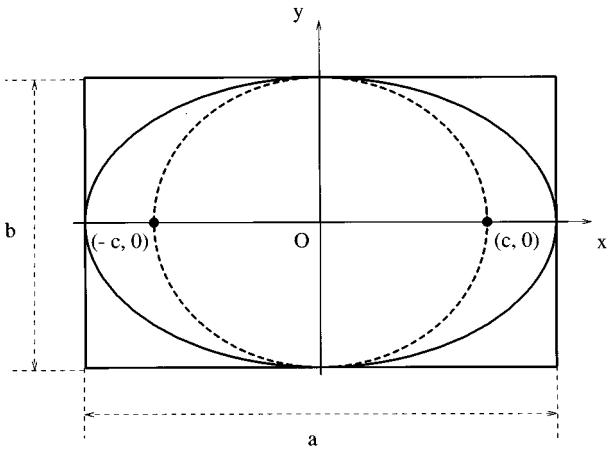

FIG. 2. The shape of the ellipse inside the unit cell for the maximum area fraction $f=\pi/4$. Here we also have $r_1=a/2$, $r_2=b/2$, and $a/b=\sqrt{2}$ so that $c=b/2$. This is one limiting case for the convergence of the series in (13).

$$\sigma_{2n}=\left(\frac{1}{b}\right)^{2n}\sum_{(p_1,p_2)\neq(0,0)}\left(\frac{1}{p_1a/b+ip_2}\right)^{2n}=\left(\frac{1}{b}\right)^{2n}\widetilde{\sigma}_{2n}, \tag{12}$$

where the quantities $\widetilde{\sigma}_{2n}$ are dimensionless. Thus the matrix elements (11) take the form

$$\lambda_{2j-1,2m-1}(c)=\left(\frac{2}{c}\right)^{2m+2j-2}\sum_{n=j+m}^{\infty}\binom{2n}{n+j+m-1}\times\binom{2n}{n+j-m}\left(\frac{c}{2b}\right)^{2n}\frac{2m-1}{2n}\widetilde{\sigma}_{2n}. \tag{13}$$

For large n, the lattice sums are well approximated by the nearest neighbors contribution [7], so that we have

$$\widetilde{\sigma}_{2n}\approx 2\left[\left(\frac{b}{a}\right)^{2n}+(-1)^n\right]. \tag{14}$$

The application of the ratio test to the series in (13) shows that the series converge absolutely if $c<b/2$. This means that if we use polar coordinates in (B10) and elliptical coordinates in (B14), then Rayleigh's method for rectangular arrays of elliptical cylinders may be applied only for a particular set of cross sections (see Fig. 2 for the case of a maximum area fraction $f=\pi/4$). Note that the elliptical coordinates (1–2) define a branch cut along the x axis, between the foci $(-c,0)$ and $(c,0)$. Thus when we use polar coordinates in the series expansion (B10), in addition to the restriction (B17) we also have to assume that $|\zeta|>c$. If the aspect ratio of the inclusions (r_1/r_2) is equal to the unit cell edge ratio (a/b)

$$\frac{r_1}{r_2}=\frac{a}{b}=\eta>1, \tag{15}$$

then Rayleigh's method may be applied for area fractions in the range

$$0<f<\frac{\pi}{4(\eta^2-1)}. \tag{16}$$

Consequently, for $\eta\leqslant\sqrt{2}$ we may apply Rayleigh's method for all the area fractions in the range $0<f<\pi/4$. Naturally, for $\eta>\sqrt{2}$, Eq. (16) defines a subset of the full range of area fractions for which Rayleigh's method is applicable.

A second set of relations between the coefficients $A_n^{e,o}$ and $B_n^{e,o}$ is obtained by means of the boundary conditions at the surface of the cylinder

$$V_i(\mu_0,\theta)=V_e(\mu_0,\theta), \tag{17}$$

$$\varepsilon\left.\frac{\partial V_i}{\partial\mu}\right|_{\mu=\mu_0}=\left.\frac{\partial V_e}{\partial\mu}\right|_{\mu=\mu_0}. \tag{18}$$

By substituting (3) and (4) into (17) and (18) we obtain the expressions of the coefficients $A_n^{e,o}$ and $C_n^{e,o}$ in terms of the $B_n^{e,o}$

$$A_n^e=\frac{\cosh(n\mu_0)+\varepsilon\sinh(n\mu_0)}{(1-\varepsilon)\sinh(2n\mu_0)}\left(\frac{2}{c}\right)^{2n}e^{-n\mu_0}B_n^e, \tag{19}$$

$$C_n^e=\frac{1}{(1-\varepsilon)\sinh(2n\mu_0)}\left(\frac{2}{c}\right)^{2n}B_n^e, \tag{20}$$

$$A_n^o=\frac{\varepsilon\cosh(n\mu_0)+\sinh(n\mu_0)}{(1-\varepsilon)\sinh(2n\mu_0)}\left(\frac{2}{c}\right)^{2n}e^{-n\mu_0}B_n^o, \tag{21}$$

$$C_n^o=\frac{1}{(1-\varepsilon)\sinh(2n\mu_0)}\left(\frac{2}{c}\right)^{2n}B_n^o, \tag{22}$$

for odd n. Setting $V_i(0,\theta)=0$, we find that $2C_0^e=2A_0^e+B_0^e=0$.

If we introduce the semiaxes of the ellipse

$$r_1=c\cosh\mu_0,\quad r_2=c\sinh\mu_0,\quad r_1\geqslant r_2, \tag{23}$$

and the depolarization factors [23]

$$L_1=r_1/(r_1+r_2),\quad L_2=r_2/(r_1+r_2),\quad L_1\geqslant L_2, \tag{24}$$

then the relations (19) and (21) take the form

$$A_\ell^e=\left[\frac{1+\varepsilon}{1-\varepsilon}+(L_1-L_2)^\ell\right]\frac{(2L_1)^\ell(2L_2)^\ell}{1-(L_1-L_2)^{2\ell}}\left(\frac{\pi}{fab}\right)^\ell B_\ell^e, \tag{25}$$

$$A_\ell^o=\left[\frac{1+\varepsilon}{1-\varepsilon}-(L_1-L_2)^\ell\right]\frac{(2L_1)^\ell(2L_2)^\ell}{1-(L_1-L_2)^{2\ell}}\left(\frac{\pi}{fab}\right)^\ell B_\ell^o, \tag{26}$$

for odd ℓ. Here we have also used the area fraction

$$f=\pi r_1r_2/(ab), \tag{27}$$

where a and b are the dimensions of the unit cell (see Fig. 1).

By substituting (25) and (26) into (8) and (9), respectively, we obtain two decoupled linear systems for the coefficients B_n^e and B_n^o. When $c=0$, we have $\lambda_{k,\ell}(0)=0$,

$r_1=r_2=\rho$, $L_1=L_2=1/2$, $f=\pi\rho^2/(ab)$, and we obtain the solution for a rectangular array of cylinders of radius ρ [7].

III. THE DIELECTRIC TENSOR OF DILUTE NONCRITICAL COMPOSITES

First, we consider a single elliptical cylinder subject to a uniform electric field $\mathbf{E}_0$, oriented as shown in Fig. 1. The potential of the applied field is

$$V_0(\mu,\theta)=E_0c(\cosh\mu\cos\theta\cos\gamma+\sinh\mu\sin\theta\sin\gamma), \tag{28}$$

and the potentials in the region exterior to the cylinder (V_e) and inside the cylinder (V_i) have the forms (3) and (4), respectively. In addition to the boundary conditions (17) and (18) the potential V_e has to satisfy the relation [24]

$$V_e(\mu,\theta)\big|_{\mu\to\infty}=V_0(\mu,\theta). \tag{29}$$

From (3) and (29) we obtain

$$A^e_{\ell}=E_0\cos\gamma\,\delta_{\ell,1}, \tag{30}$$

$$A^o_{\ell}=E_0\sin\gamma\,\delta_{\ell,1}, \tag{31}$$

so that the only nonzero coefficients in the series expansion of the response field are

$$B^e_1=\frac{(1-\varepsilon)\sinh(2\mu_0)}{\cosh\mu_0+\varepsilon\sinh\mu_0}\left(\frac{c}{2}\right)^2 e^{\mu_0}E_0\cos\gamma, \tag{32}$$

$$B^o_1=\frac{(1-\varepsilon)\sinh(2\mu_0)}{\varepsilon\cosh\mu_0+\sinh\mu_0}\left(\frac{c}{2}\right)^2 e^{\mu_0}E_0\sin\gamma. \tag{33}$$

Due to the anisotropy of the system, the relation between the polarization of the cylinder and the applied field has the form [24,25]

$$\begin{pmatrix}P_1\\P_2\end{pmatrix}=-2\pi\varepsilon_0\begin{pmatrix}\alpha_{11}&0\\0&\alpha_{22}\end{pmatrix}\begin{pmatrix}E_{0,1}\\E_{0,2}\end{pmatrix}, \tag{34}$$

where the labels 1 and 2 specify the x and y components of the vectors $\mathbf{P}$ and $\mathbf{E}_0$, and the minus sign has been introduced according to the orientation of the applied field. The nonzero components of the polarizability tensor ($\ddot{\alpha}$) are given by the formulas

$$\alpha_{11}=-\frac{P_1}{2\pi\varepsilon_0E_{0,1}}=-\frac{B^e_1}{A^e_1}=\frac{\varepsilon-1}{L_1+\varepsilon L_2}\frac{fab}{2\pi}, \tag{35}$$

$$\alpha_{22}=-\frac{P_2}{2\pi\varepsilon_0E_{0,2}}=-\frac{B^o_1}{A^o_1}=\frac{\varepsilon-1}{\varepsilon L_1+L_2}\frac{fab}{2\pi}. \tag{36}$$

Now, for a dilute composite we may use the Clausius-Mossotti formula to obtain the components of the dielectric tensor

$$\frac{\varepsilon^*_{jj}-1}{\varepsilon^*_{jj}+1}=\pi\alpha_{jj}n,\quad j=1,2 \tag{37}$$

where $n=1/(ab)$ is the number of cylinders per unit area. The off-diagonal elements of $\ddot{\varepsilon}^*$ are zero. From (37), by using the relation $L_1+L_2=1$, we obtain Galeener's formula [18,19]

$$\frac{\varepsilon^*_{jj}-1}{\varepsilon^*_{jj}+1}=\frac{f}{2}\frac{\varepsilon-1}{L_j+(1-L_j)\varepsilon},\quad j=1,2 \tag{38}$$

or

$$\varepsilon^*_{jj}=1-\frac{2f}{\dfrac{1+\varepsilon}{1-\varepsilon}+(2L_j-1)+f},\quad j=1,2. \tag{39}$$

If, for the same problem of a dilute composite, we use the Rayleigh identity in the first approximation, the linear systems (8) and (9) take the form

$$\left\{\left[\frac{1+\varepsilon}{1-\varepsilon}+(L_1-L_2)\right]\frac{\pi}{fab}+\sigma_2(\gamma_1)+\lambda_{1,1}(c)\right\}B^e_1=E_0\cos\gamma, \tag{40}$$

$$\left\{\left[\frac{1+\varepsilon}{1-\varepsilon}+(L_2-L_1)\right]\frac{\pi}{fab}-\sigma_2(\gamma_2)-\lambda_{1,1}(c)\right\}B^o_1=E_0\sin\gamma. \tag{41}$$

Here, we have also used the relations (25) and (26). Equations (40) and (41) correspond to two problems: (i) a rectangular array of elliptical cylinders with the applied field along the negative x axis ($E_{0,1}=E_0\cos\gamma$), and (ii) a rectangular array of elliptical cylinders with the applied field along the negative y axis ($E_{0,2}=E_0\sin\gamma$). In both cases we have the same orientation of the axes, the unit cell having the longer edge along the x axis ($a>b$). The lattice sum σ_2 has to be evaluated over a needle-shaped region elongated in the direction of the applied field [4,5,11,12], so that we have to use $\gamma_1=0$ in (40) and $\gamma_2=\pi/2$ in (41). This indicates a rotation of the applied field by an angle of $\pi/2$ between (40) and (41). In conclusion, the two Eqs. (40) and (41) describe the problems shown in Fig. 3(A) and Fig. 3(B), respectively.

The sum $\lambda_{1,1}(c)$ has the expression

$$\lambda_{1,1}(c)=\sum_{n=2}^{\infty}\binom{2n}{n+1}\binom{2n}{n}\left(\frac{c}{2}\right)^{2n-2}\frac{\sigma_{2n}}{2n}=\frac{3}{2}\sigma_4c^2+O(c^4), \tag{42}$$

and

$$c^2=|r_1^2-r_2^2|. \tag{43}$$

Therefore, when c is small, to order f we may neglect $\lambda_{1,1}(c)$ in (40) and (41). In this approximation the components of the dielectric tensor are [4]

$$\varepsilon^*_{11}=1-2\pi\frac{B^e_1}{abE_{0,1}}=1-\frac{2f}{\dfrac{1+\varepsilon}{1-\varepsilon}+(L_1-L_2)+fab\sigma_2(0)/\pi}, \tag{44}$$

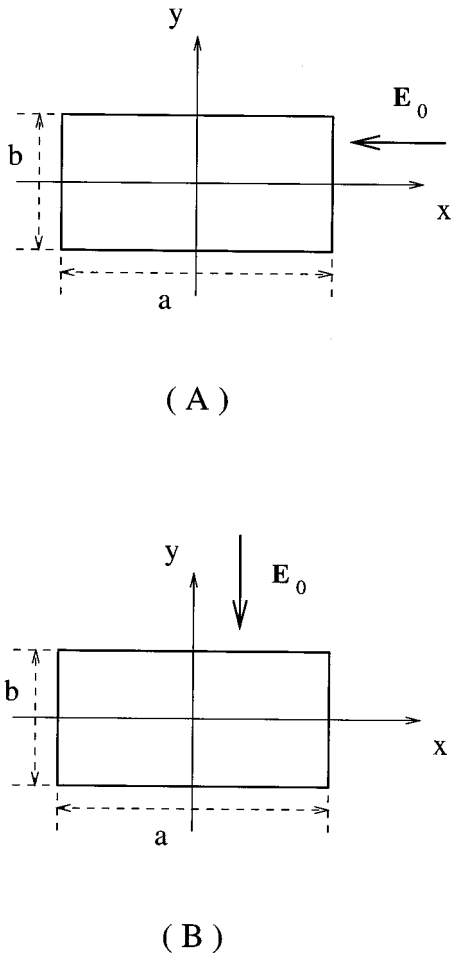

FIG. 3. The physical systems described by (40) and (41) and (58) and (59).

$$\varepsilon_{22}^{*}=1-2\pi\frac{B_1^o}{abE_{0,2}}$$
$$=1-\frac{2f}{\frac{1+\varepsilon}{1-\varepsilon}+(L_2-L_1)-fab\sigma_2(\pi/2)/\pi}. \quad (45)$$

Note the difference between (39) and (44) and (45) in the coefficient of f in the denominator. Only in the case of a square array ($a=b$), by means of the formula [14]

$$\sigma_2(\gamma)=-\frac{\pi}{a^2}e^{-2i(\gamma+\pi/2)}, \quad (46)$$

we obtain $\sigma_2(0)=-\sigma_2(\pi/2)=\pi/(ab)$, so that $\tilde{\varepsilon}^*$ obtained from the first approximation of Rayleigh's identity coincides with Galeener's result for a circular Lorentz cavity. Cohen *et al.* [20] discussed what they viewed as inconsistencies arising from Galeener's formula, and derived a formula based on an elliptical Lorentz cavity having the same depolarization factors as the inclusions

$$\varepsilon_{jj}^{*}=1-\frac{2f}{\frac{1+\varepsilon}{1-\varepsilon}+(2L_j-1)+2f(1-L_j)}, \quad j=1,2. \quad (47)$$

The expression (47) for $\tilde{\varepsilon}^*$ also differs from (44) and (45) even for a square array. This is not surprising, given that any argument with an answer involving a depolarization factor for the Lorentz cavity, as distinct from the particle, is not rigorous. Rayleigh's theory takes into account both the shape of the inclusions, by means of the depolarization factors, and the geometry of the array, by means of the lattice sums. It also includes the direction of the incident field in the evaluation of the lattice sum σ_2. In general, for a rectangular array we have [14]

$$\sigma_2(\gamma)=\lim_{k\to 0}\frac{S_2^Y(k,0)}{Y_2(k)}-\frac{\pi}{ab}e^{-2i(\gamma+\pi/2)}. \quad (48)$$

Here, S_2^Y is a dynamic lattice sum which has the representation

$$S_2^Y(k,0)J_2(k\xi)=\frac{4}{ab}\sum_h\frac{J_2(K_h\xi)}{K_h^2-k^2}e^{-i\theta_h}, \quad (49)$$

where $\boldsymbol{\xi}$ is a vector in the central unit cell and $\mathbf{K}_h$, $h\in\mathbb{Z}^2$, are the reciprocal array vectors [in polar coordinates $\mathbf{K}_h=(K_h,\theta_h)$]. Also, J_2 and Y_2 represent Bessel functions of the first and second kind, respectively. In Table I we give the values of $\sigma_2(\gamma)$ as a function of a/b, for $\gamma=0$ and $\gamma=\pi/2$. The first term in (48) vanishes in the case of a square or hexagonal array. Therefore, if $a=b=1$, we have $\sigma_2(0)=-\sigma_2(\pi/2)=\pi$ (see the first line in Table I).

The series in (49) are absolutely convergent, and the first term in (48) is independent of γ. Therefore, the lattice sums $\sigma_2(\gamma)$ satisfy the relation

$$\sigma_2(0)-\sigma_2(\pi/2)=\frac{2\pi}{ab}. \quad (50)$$

A numerical check of (50) is given in the last two columns of Table I. Here, we have used $b=1$ and $a\geqslant b$. It can be seen that relation (50) is satisfied numerically with an accuracy of 10^{-9} (nine decimal places).

Also, the method used by Lord Rayleigh [4] to evaluate $\sigma_2(\pi/2)$ gives us the value

$$\sigma_2(\pi/2)\approx-\frac{\pi^2}{3}\approx-3.289\,868\,134, \quad (51)$$

for $a\gg b=1$. Consequently, in this limit we have

$$\sigma_2(0)\approx\frac{2\pi}{a}-\frac{\pi^2}{3}. \quad (52)$$

Note that, from Table I, $\sigma_2(\pi/2)=-\pi^2/3$ (to ten figures) for values of a/b greater than or equal to 5. In this range, we can use (52) to give $\sigma_2(0)$ to the same accuracy.

In the case of a rectangular array of circular cylinders, touching in one direction [$r_1=r_2=\min(a,b)/2$], the rows of cylinders are similar with an effective slab of the same ma-

TABLE I. The lattice sum $\sigma_2(\gamma)$ evaluated from (48), for different values of a/b. Here, we have used $b=1$. The last two columns represent the left and right sides of (50).

a/b	$\gamma=0$	$\gamma=\pi/2$	$\sigma_2(0)-\sigma_2(\pi/2)$	$2\pi/(ab)$
1	3.141 592 654	−3.141 592 654	6.283 185 307	6.283 185 307
$\sqrt{2}$	1.163 942 558	−3.278 940 380	4.442 882 938	4.442 882 938
2	−0.148 000 128	−3.289 592 781	3.141 592 654	3.141 592 654
3	−1.195 472 517	−3.289 867 619	2.094 395 102	2.094 395 102
4	−1.719 071 806	−3.289 868 133	1.570 796 327	1.570 796 327
5	−2.033 231 072	−3.289 868 134	1.256 637 061	1.256 637 061
6	−2.242 670 582	−3.289 868 134	1.047 197 551	1.047 197 551
7	−2.392 270 233	−3.289 868 134	0.897 597 901	0.897 597 901
8	−2.504 469 970	−3.289 868 134	0.785 398 163	0.785 398 163
9	−2.591 736 433	−3.289 868 134	0.698 131 701	0.698 131 701
10	−2.661 549 603	−3.289 868 134	0.628 318 531	0.628 318 531
15	−2.870 989 113	−3.289 868 134	0.418 879 020	0.418 879 020
20	−2.975 708 868	−3.289 868 134	0.314 159 265	0.314 159 265

terial. With the lattice sum $\sigma_2(\gamma)$ given by (48), the results from (44) and (45) agree completely with the results obtained by Ninham and Sammut [7,26].

IV. THE DIELECTRIC TENSOR OF DILUTE CRITICAL COMPOSITES

Here, we will consider a special type of rectangular array of elliptical cylinders, having $r_1/a\to 0$ and $2r_2/b\to 1$ (see Fig. 4). This is a composite with a very small area fraction but with important multipole effects. In this case $c\approx r_2$ and, in the first order approximation of Rayleigh's identity (40) and (41), we cannot neglect the series $\lambda_{1,1}(c)$. Thus we obtain the Maxwell-Garnett type formulas

$$\varepsilon_{11}^{*}=1-\frac{2f}{\dfrac{1+\varepsilon}{1-\varepsilon}+(L_1-L_2)+\dfrac{fab}{\pi}[\sigma_2(0)+\lambda_{1,1}(c)]}, \tag{53}$$

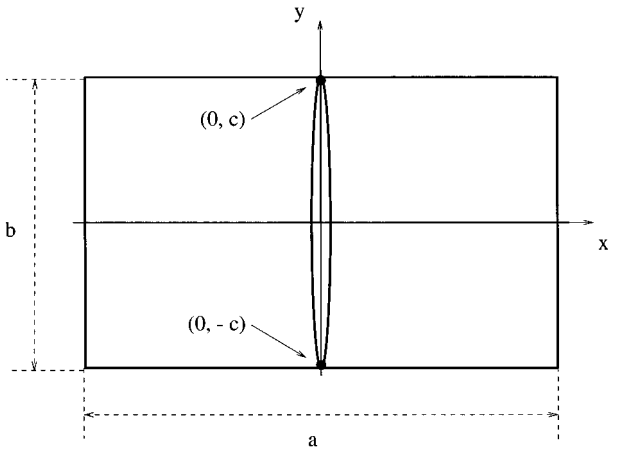

FIG. 4. An ellipse elongated along the y axis, inside the unit cell, for $a=5$, $b=1$, $r_1=a/50$, and $r_2\lesssim b/2$. The area fraction is $f\approx\pi/100$. Here, we also have $r_1<<r_2$ so that $c\lesssim b/2$.

$$\varepsilon_{22}^{*}=1-\frac{2f}{\dfrac{1+\varepsilon}{1-\varepsilon}+(L_2-L_1)-\dfrac{fab}{\pi}[\sigma_2(\pi/2)+\lambda_{1,1}(c)]}. \tag{54}$$

At the same time, f is small and higher order truncation orders of (8) and (9) will give results almost identical with (53) and (54).

In Figs. 5(A) and 5(B) we show the dependence of ε_{11}^{*} and ε_{22}^{*} on r_2, for a rectangular array of perfectly conducting ($\varepsilon\to\infty$) elliptical cylinders, with $a/b=2$, $b=1$, and $r_1=a/100$. It can be seen that, in the limit of graphical accuracy, the curves for truncation orders 1, 10, and 20 coincide. For ε_{11}^{*} the dependence on r_2 is almost linear, as the distance between the cylinders, along the x axis, is $\approx 2a$ (much larger than r_1). Note that as $r_2\to 0$ the numerical results from the Rayleigh identity differ from 1. Actually, as r_2 approaches zero we have a rectangular array of perfectly conducting thin strips of width $2r_1$ and therefore, the dielectric constant of the array never equals the dielectric constant of the matrix. From (53) we obtain

$$\varepsilon_{11}^{*}=1+\frac{2\pi r_1^2/(ab)}{2-r_1^2[\sigma_2(0)+\lambda_{1,1}(r_1)]}\approx 1+\pi\left(\frac{r_1}{a}\right)^2\left(\frac{a}{b}\right)$$
$$=1.000\,628. \tag{55}$$

In contrast with this result, for a rectangular array of perfectly conducting circular cylinders, $\varepsilon_{11}^{*}\to 1$ as the radius of the cylinders tends to zero [see Fig. 5(A)].

The dielectric constant ε_{22}^{*}, for the incident field along the y axis, exhibits a similar behavior for a rectangular array of perfectly conducting elliptical cylinders and a rectangular array of perfectly conducting circular cylinders, of radius r_2. Even the Maxwell-Garnett type formula (54) gives high values of ε_{22}^{*} when the ellipses are close to touching along the y axis. The maximum values of ε_{22}^{*} are well approximated if we consider a series of capacitors along the y axis [5,27].

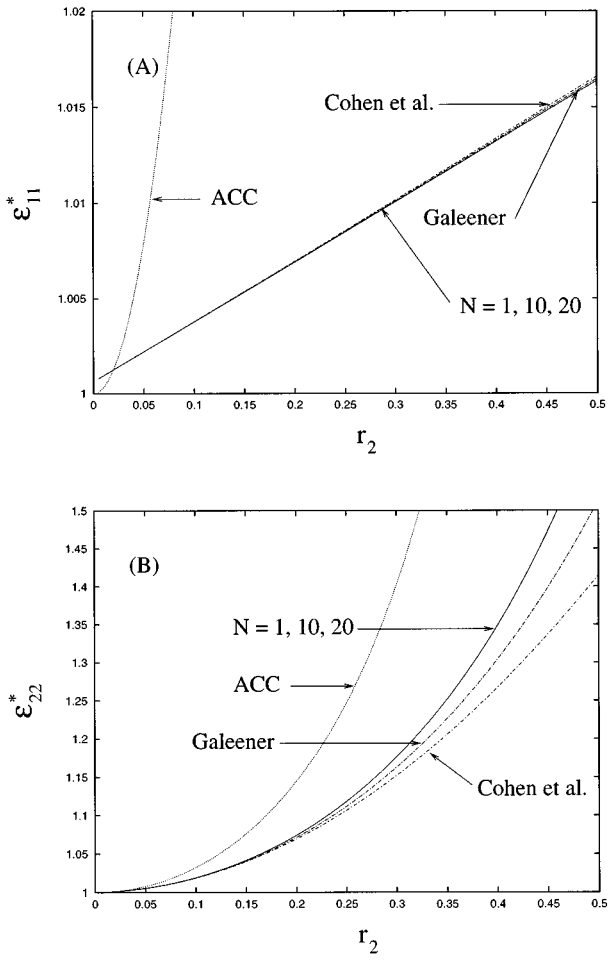

FIG. 5. The components of the dielectric tensor ε^*_{11} (A) and ε^*_{22} (B), as functions of r_2, for different truncation orders (N) of (8) and (9), for a rectangular array of perfectly conducting elliptical cylinders. The unit cell of the array has the edges $a=2$, $b=1$ and the minor semiaxis of the ellipses is $r_1=a/100$. We also show the results from the formulas derived by Galeener (39) [18] and Cohen *et al.* (47) [20], and the components of the dielectric tensor for the rectangular array with perfectly conducting circular cylinders of radius r_2 (ACC).

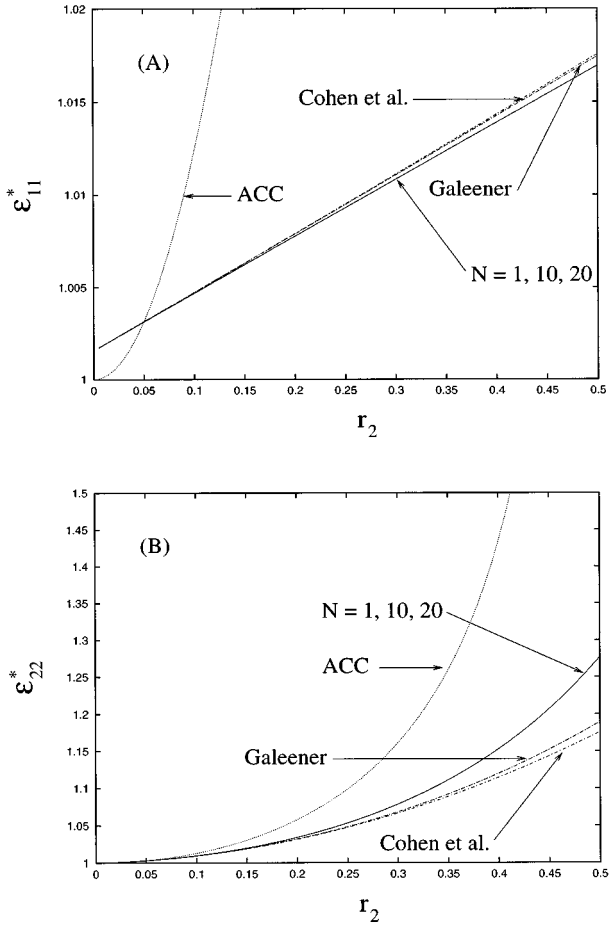

FIG. 6. The components of the dielectric tensor ε^*_{11} (A) and ε^*_{22} (B), as functions of r_2, for different truncation orders (N) of (8) and (9), for a rectangular array of perfectly conducting elliptical cylinders. The unit cell of the array has the edges $a=5$, $b=1$ and the minor semiaxis of the ellipses is $r_1=a/100$. We also show the results from the formulas derived by Galeener (39) [18] and Cohen *et al.* (47) [20], and the components of the dielectric tensor for the rectangular array with perfectly conducting circular cylinders of radius r_2 (ACC).

We also show in Figs. 5(A) and 5(B) the numerical results obtained from the Maxwell-Garnett type formulas derived by Galeener (39) [18] and Cohen *et al.* (47) [20]. The corresponding curves for ε^*_{22} are similar and both differ from the results obtained from the Rayleigh identity.

In Figs. 6(A) and 6(B) we give the results from a similar analysis for a rectangular array of perfectly conducting elliptical cylinders having $r_1=a/100$ and $b=1$, but with $a/b=5$. In this case we have a behavior of ε^*_{11} as a function of r_2 similar to that shown in Fig. 5(A). Now, the curves of ε^*_{22}, as a function of r_2, for different truncation orders are identical, to the limit of graphical accuracy [see Fig. 6(B)], but they are not so close to the curve corresponding to a rectangular array of perfectly conducting circular cylinders of radius r_2 [compare Fig. 6(B) and Fig. 5(B)]. Again, the ε^*_{22} curves from the formulas (39) and (47) give completely different results.

V. THE DIELECTRIC TENSOR OF CONCENTRATED COMPOSITES

In the case of a concentrated composite we may find the dielectric tensor from the equations [4]

$$\varepsilon^*_{11}=1-2\pi\frac{B^e_1}{abE_{0,1}}, \tag{56}$$

$$\varepsilon^*_{22}=1-2\pi\frac{B^o_1}{abE_{0,2}}, \tag{57}$$

with B^e_1 and B^o_1 obtained by solving the linear systems

$$\left[\frac{1+\varepsilon}{1-\varepsilon}+(L_1-L_2)^{\ell}\right]\frac{(2L_1)^{\ell}(2L_2)^{\ell}}{1-(L_1-L_2)^{2\ell}}\left(\frac{\pi}{fab}\right)^{\ell}B^e_{\ell}$$

$$+\sum_{m\ \mathrm{odd}}\Lambda_{\ell,m}(c)B^e_m=E_0\cos\gamma\delta_{\ell,1}, \tag{58}$$

$$\left[\frac{1+\varepsilon}{1-\varepsilon}-(L_1-L_2)^{\ell}\right]\frac{(2L_1)^{\ell}(2L_2)^{\ell}}{1-(L_1-L_2)^{2\ell}}\left(\frac{\pi}{fab}\right)^{\ell}B^o_{\ell}$$

$$-\sum_{m\ \text{odd}}\Lambda_{\ell,m}(c)B^o_m=E_0\sin\gamma\,\delta_{\ell,1}, \tag{59}$$

for odd ℓ. Here, as in the case of dilute composites, we have to use the lattice sum $\sigma_2(0)$ in (58) and $\sigma_2(\pi/2)$ in (59). All the other lattice sums in (59) are identical with the corresponding lattice sums from (58). Note that, of all the coefficients $\Lambda_{i,j}(c)$, as defined in (10), only $\Lambda_{1,1}(c)$ contains the lattice sum σ_2. Also none of the coefficients $\lambda_{i,j}(c)$ depend on σ_2.

To evaluate numerically the components of the dielectric tensor we introduce the variables

$$B^e_n=\frac{E_0\cos\gamma}{\sqrt{n}}\sqrt{\frac{1-(L_1-L_2)^{2n}}{(2L_1)^n(2L_2)^n}\left(\frac{fab}{\pi}\right)^n}\,Q^e_n, \tag{60}$$

$$B^o_n=\frac{E_0\sin\gamma}{\sqrt{n}}\sqrt{\frac{1-(L_1-L_2)^{2n}}{(2L_1)^n(2L_2)^n}\left(\frac{fab}{\pi}\right)^n}\,Q^o_n, \tag{61}$$

so that the systems (58) and (59) may be written in the matrix form

$$[\mathbf{D}^e+\mathbf{W}]\mathbf{Q}^e=\mathbf{U}, \tag{62}$$

$$[\mathbf{D}^o-\mathbf{W}]\mathbf{Q}^o=\mathbf{U}, \tag{63}$$

where $\mathbf{D}^{e,o}$ are diagonal matrices with the nonzero elements

$$d^e_{\ell\ell}=\frac{1+\varepsilon}{1-\varepsilon}+(L_1-L_2)^{\ell}, \tag{64}$$

$$d^o_{\ell\ell}=\frac{1+\varepsilon}{1-\varepsilon}-(L_1-L_2)^{\ell}, \tag{65}$$

$\mathbf{U}$ is a vector with only one nonzero component ($u_1=\sqrt{r_1r_2}$) and the matrix $\mathbf{W}$ has the elements

$$w_{\ell,m}=\Lambda_{\ell,m}(c)\sqrt{\frac{\ell}{m}}\left(\frac{r_1+r_2}{2}\right)^{\ell+m}$$
$$\times\sqrt{[1-(L_1-L_2)^{2\ell}][1-(L_1-L_2)^{2m}]}. \tag{66}$$

If the dielectric constant of the cylinders (ε) is real, then the matrices

$$\mathbf{M}^{e,o}=\mathbf{D}^{e,o}\pm\mathbf{W}, \tag{67}$$

are real and symmetric. By truncating the linear systems (62) and (63) at some finite order N, and solving for the unknowns $\mathbf{Q}^{e,o}$, we obtain the components of the dielectric tensor from the equations

$$\varepsilon^*_{11}=1-2\left(\frac{f\pi}{ab}\right)^{1/2}Q^e_1, \tag{68}$$

$$\varepsilon^*_{22}=1-2\left(\frac{f\pi}{ab}\right)^{1/2}Q^o_1. \tag{69}$$

Note that all the eigenvalues of the matrices (67) are real. If we truncate $\mathbf{M}^{e,o}$ at some finite order N we may reduce these matrices to the diagonal form by orthogonal similarity transformations. Denoting the eigenvalues of $\mathbf{M}^e$ and $\mathbf{M}^o$ by ω^e_k and ω^o_k, respectively, the components of the dielectric tensor are given by the formulas [6]

$$\varepsilon^*_{11}=1-2f\sum_{k=1}^{N}\frac{(v^e_{1,k})^2}{\omega^e_k}, \tag{70}$$

$$\varepsilon^*_{22}=1-2f\sum_{k=1}^{N}\frac{(v^o_{1,k})^2}{\omega^o_k}. \tag{71}$$

Here, v^e_{1k} and v^o_{1k} represent the first component of the kth eigenvector of $\mathbf{M}^e$ and $\mathbf{M}^o$, respectively. Numerically, we have to reduce the initial real symmetric matrix to tridiagonal form by Householder's algorithm. Then we may use the QL algorithm with implicit shifts to find the eigenvalues of the reduced matrix [28]. In practice, for high truncation orders N this method proved to be more stable than the method of solving (62) and (63) by direct inversion of (67).

The components of the dielectric tensor satisfy Keller's theorem [30]

$$\varepsilon^*_{11}(\varepsilon)\varepsilon^*_{22}(1/\varepsilon)=1. \tag{72}$$

This property is a consequence of the algebraic structure of the linear systems (62) and (63), and it is true for arbitrary truncation orders N. Thus in checking numerical results Eq. (72) represents only a necessary condition, not a sufficient condition [5]. Note that *all* the formulas (39), (44) and (45), and (47) satisfy Keller's theorem.

The Rayleigh identities (62) and (63) may be used for a limited range of area fractions, for which $c<b/2$. Under this restriction, by using the Rayleigh method in the case of a rectangular array of perfectly conducting elliptical cylinders, with $r_1/r_2=a/b=2$, we have obtained the agreement with the results of Lu [29] (all four figures given being in agreement).

If the aspect ratio of the inclusions is equal to the ratio of the edges of the unit cell, and

$$\frac{r_1}{r_2}=\frac{a}{b}=\sqrt{2}, \tag{73}$$

then we may use the Rayleigh identities (62) and (63) for the whole range of area fractions $0<f<\pi/4$, from a dilute noncritical composite (with the inclusions having a small c) to a concentrated composite when the inclusions tend to touching simultaneously in both directions, along the x and y axes. Thus, in Figs. 7(A) and 7(B) we show the behavior of ε^*_{11} and ε^*_{22}, as functions of area fraction f, for a rectangular array of perfectly conducting elliptical cylinders. The unit cell of the array has the edges $a=\sqrt{2}$ and $b=1$. The semiaxes of the cross sections of the cylinders are

$$r_1=a\sqrt{f/\pi},\quad r_2=b\sqrt{f/\pi}. \tag{74}$$

For different truncation orders of the linear systems (62) and (63), the corresponding curves differ significantly for $f\gtrsim 0.5$. A high truncation order ($N=20$) is necessary to

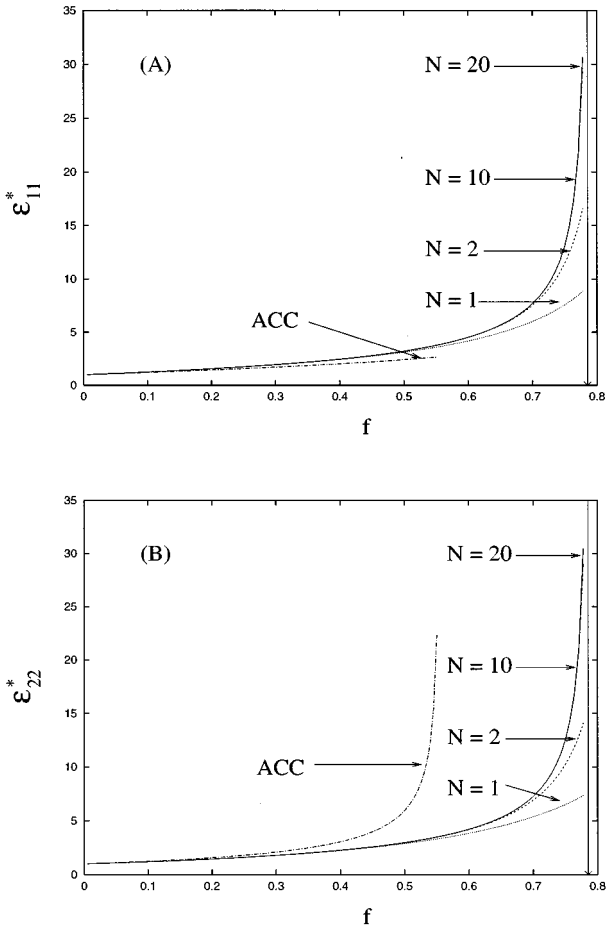

FIG. 7. The components of the dielectric tensor ε^*_{11} (A) and ε^*_{22} (B), as functions of area fraction (f), for different truncation orders (N) of (62) and (63), for a rectangular array of perfectly conducting elliptical cylinders. The unit cell of the array has the edges $a=\sqrt{2}$, $b=1$ and the aspect ratio of the ellipses is $r_1/r_2=a/b$. We also show the components of the dielectric tensor for the rectangular array with perfectly conducting circular cylinders (ACC). The vertical solid line marks the maximum area fraction $f_{\max}=\pi/4$.

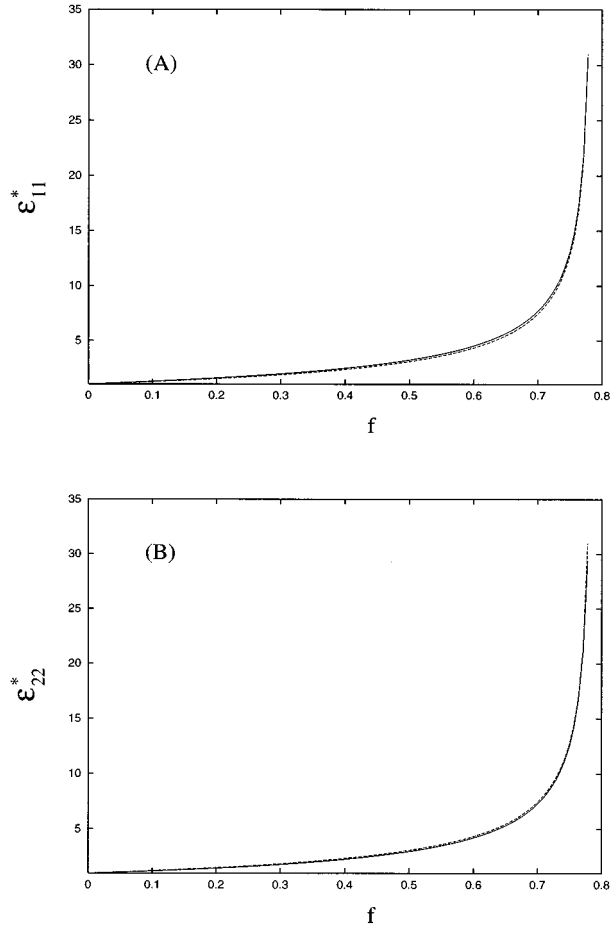

FIG. 8. The components of the dielectric tensor ε^*_{11} (A) and ε^*_{22} (B), as functions of area fraction (f), for a rectangular array of perfectly conducting elliptical cylinders (solid curves) and for a square array of perfectly conducting circular cylinders (dashed curves). The unit cell of the rectangular array has the edges $a=\sqrt{2}$, $b=1$ and the aspect ratio of the ellipses is $r_1/r_2=a/b$. The unit cell of the square array has the edge $d=1$. In both cases we have used a truncation order $N=40$.

show the divergence of ε^*_{11} and ε^*_{22} in the vicinity of $f\lesssim\pi/4$, where the cylinders are close to touching.

We also show in Figs. 7(A) and 7(B) the components of the dielectric tensor for the same rectangular array ($b=1$, $a=\sqrt{2}$) but with perfectly conducting circular cylinders of radius $r_2=\sqrt{fab/\pi}$. The corresponding curves stop at $r_2\lesssim b/2$, when the cylinders are close to touching along the y axis [maximum area fraction $f=\pi/(4\sqrt{2})\approx 0.555$]. For such a composite $\varepsilon^*_{22}\to\infty$ as $r_2\to b/2$ [see Fig. 7(B)], while ε^*_{11} has a finite value [see Fig. 7(A)].

In Figs. 8(A) and 8(B) we compare the components of the dielectric tensor for a *rectangular array* of perfectly conducting elliptical cylinders and the dielectric constant of a *square array* of perfectly conducting circular cylinders. The unit cell of the rectangular array has the edges $a=\sqrt{2}$ and $b=1$, and the semiaxes of the ellipses are given by (74). The square array has the edge of the unit cell $d=1$ and the radius of the cylinders is given by $r=d\sqrt{f/\pi}$. As functions of area fraction ε^*_{11} and ε^*_{22} for the rectangular array coincide (in the limit of graphical accuracy) with the dielectric constant for the square array. This means that all these quantities are determined by the relative gap between the inclusions (g_x and g_y for the rectangular array, and g for the square array). Thus for elliptical cylinders in a rectangular array we have

$$g_x=\frac{a-2r_1}{a}=1-2\frac{r_1}{a}, \tag{75}$$

$$g_y=\frac{b-2r_2}{b}=1-2\frac{r_2}{b}, \tag{76}$$

where $r_1/a=r_2/b=\sqrt{f/\pi}$, so that $g_x=g_y$. For circular cylinders in a square array the relative gap is the same along the x and y axes

$$g=1-2\frac{r}{d}=1-2\sqrt{f/\pi}. \tag{77}$$

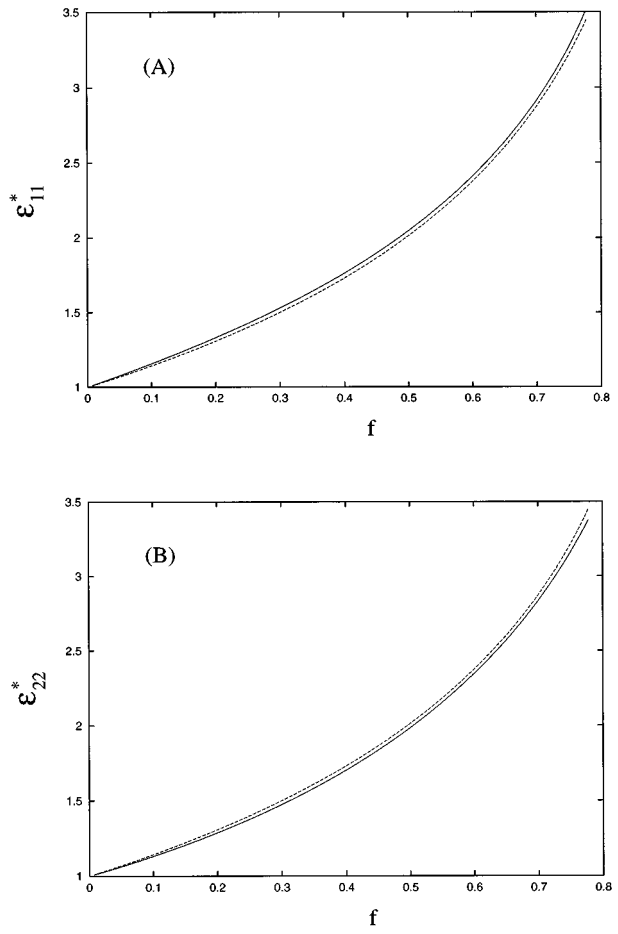

FIG. 9. The components of the dielectric tensor ε^*_{11} (A) and ε^*_{22} (B), as functions of area fraction (f), for a rectangular array of elliptical cylinders (solid curves) and for a square array of circular cylinders (dashed curves). The relative dielectric constant of the inclusions is $\varepsilon=5$. The unit cell of the rectangular array has the edges $a=\sqrt{2}$, $b=1$ and the aspect ratio of the ellipses is $r_1/r_2=a/b$. The unit cell of the square array has the edge $d=1$. In both cases we have used a truncation order $N=40$.

Consequently, the relative gap is the same along the x and y axes for both systems, and therefore the dielectric constant is similar for both directions and systems.

In Figs. 9(A) and 9(B) we compare the components of the dielectric tensor for a rectangular array of elliptical cylinders and the dielectric constant of a square array of circular cylinders. The geometry of the arrays is the same as in Fig. 8, but the relative dielectric constant of the inclusions is $\varepsilon=5$. It can be seen that, due to the particular value of the aspect ratio of the inclusions and the geometry of the rectangular array, there are quite small differences between ε^*_{11} and ε^*_{22} for the rectangular array and the dielectric constant of the square array, over the whole range of area fractions $0<f<\pi/4$.

VI. CONCLUSIONS

We have extended the Rayleigh method [4] for inclusions with noncircular boundaries. This extension is a hybrid technique: the lattice sums are evaluated in polar coordinates, while for the boundary conditions we use elliptical coordinates. By means of our technique we have analyzed numerically and analytically three types of composites: dilute noncritical, dilute critical, and concentrated. For dilute noncritical and dilute critical composites we have obtained different Maxwell-Garnett type formulas. Note that our dipole formula for dilute critical composites works well even when $|\varepsilon^*|\gg 1$. Previous asymptotic analysis of composites has relied on methods other than the application oflRow order Rayleigh identities.

The hybrid technique is limited by geometrical constraints, so that it may be applied only for a limited range of area fractions. Even with these limitations, the Rayleigh method represents an excellent mathematical formalism for analytical studies. In future work we will develop a method in which both the lattice sums and the boundary conditions are represented in the same coordinate system. We will also attempt to remove the restriction that the axes of the ellipses and of the array coincide.

ACKNOWLEDGMENTS

This work was supported by the Australian Research Council, from the Department of Employment, Education, and Training. This body also provided computing facilities. The Science Foundation for Physics within the University of Sydney is also acknowledged.

APPENDIX A: POTENTIAL EXPANSIONS

Expressions (3) and (4) for the potential outside and inside the cylinder differ from the corresponding potential expansions used by Morse and Feshbach [21]. The coefficients have been chosen so that, in the limit $c\to 0$, when the ellipse is transformed into a circle, the potential takes the usual form in polar coordinates. This form is obtained by means of the limits [22]

$$\lim_{\substack{c\to 0\\ \mu\to\infty}} \frac{c}{2}e^{\mu}=r, \quad \lim_{\substack{c\to 0\\ \mu\to\infty}} \frac{c}{2}e^{-\mu}=0, \quad \lim_{\substack{c\to 0\\ \mu\to\infty}} \frac{2}{c}e^{-\mu}=\frac{1}{r}, \tag{A1}$$

where r is the distance to the origin in polar coordinates. Also, the coordinate θ becomes the polar angle φ. Consequently, from (3) and (4) we have

$$V_e(r,\varphi)=2A_0^e+B_0^e+\sum_{n=1}^{\infty}\{[A_n^e r^n+B_n^e r^{-n}]\cos(n\varphi) +[A_n^o r^n+B_n^o r^{-n}]\sin(n\varphi)\}, \tag{A2}$$

in the matrix ($r\geqslant r_0$), and

$$V_i(\mu,\varphi)=2C_0^e+\sum_{n=1}^{\infty}[C_n^e r^n\cos(n\varphi)+C_n^o r^n\sin(n\varphi)], \tag{A3}$$

inside the cylinder ($0\leqslant r\leqslant r_0$). Therefore the coefficients $A_n^{e,o}$, $B_n^{e,o}$ and $C_n^{e,o}$ have the same dimension in elliptical coordinates as in polar coordinates.

APPENDIX B: THE GREEN'S FUNCTION

We consider the problem of a uniform electric field applied to a periodic array of elliptical cylinders. The centers of the cylinders are specified by the array vectors

$$\mathbf{R}_p = p_1\hat{\mathbf{e}}_1 + p_2\hat{\mathbf{e}}_2, \quad p=(p_1,p_2)\in\mathbb{Z}^2, \tag{B1}$$

where $\hat{\mathbf{e}}_1$ and $\hat{\mathbf{e}}_2$ represent the fundamental translation vectors of the array.

The Green's function for our problem is the solution of the Poisson equation

$$\nabla^2 G(\mathbf{r};\mathbf{r}_0) = -2\pi\sum_p \delta(\mathbf{r}-\mathbf{r}_0-\mathbf{R}_p), \tag{B2}$$

and has the form

$$G(\mathbf{r};\mathbf{r}_0) = -\ln|\mathbf{r}-\mathbf{r}_0| - \sum_{p\neq 0} \ln\frac{|\mathbf{r}-\mathbf{r}_0-\mathbf{R}_p|}{R_p}. \tag{B3}$$

By introducing the representation in the complex plane of the vectors involved in (B3), the Green's function takes the form

$$G(z;z_0) = G_0(z;z_0) + \sum_{p\neq 0} G_p(z;z_0), \tag{B4}$$

where

$$G_0(z;z_0) = -\mathrm{Re}\,\ln(z-z_0), \tag{B5}$$

$$G_p(z;z_0) = -\mathrm{Re}\,\ln\frac{z-z_0-z_p}{z_p}. \tag{B6}$$

Now, we consider the transform to elliptical coordinates defined by $z=c\cosh w$, with $w=\mu+i\theta$. In Cartesian coordinates, this transform is given by Eqs. (1) and (2). We also have $z_0=c\cosh w_0$ and, by substituting in (B5), we obtain [21]

$$\begin{aligned}-\ln(z-z_0) &= -\ln(c\cosh w - c\cosh w_0)\\ &= -\ln\frac{c}{2} - w + 2\sum_{n=1}^{\infty}\frac{e^{-nw}}{n}\cosh(nw_0),\end{aligned} \tag{B7}$$

for $|w|>|w_0|$. Hence for $\mu>\mu_0$, we have

$$\begin{aligned}G_0(z;z_0) = &-\ln\frac{c}{2} - \mu\\ &+ 2\sum_{n=1}^{\infty}\frac{e^{-n\mu}}{n}[\cosh(n\mu_0)\cos(n\theta_0)\cos(n\theta)\\ &+ \sinh(n\mu_0)\sin(n\theta_0)\sin(n\theta)].\end{aligned} \tag{B8}$$

To obtain the series expansion of (B6) we denote by $\zeta=z-z_0$. If ζ is restricted to the unit cell, so that

$$|\zeta|<|z_p|, \quad \forall p\neq 0 \tag{B9}$$

we have

$$-\ln\frac{z-z_0-z_p}{z_p} = -i\pi + \sum_{n=1}^{\infty}\frac{1}{n}\left(\frac{\zeta}{z_p}\right)^n, \tag{B10}$$

so that

$$\sum_{p\neq 0} G_p(z;z_0) = \mathrm{Re}\sum_{n=1}^{\infty}\frac{\zeta^n}{n}\sigma_n, \tag{B11}$$

where we have introduced the lattice sums

$$\sigma_n = \sum_{p\neq 0}\left(\frac{1}{z_p}\right)^n. \tag{B12}$$

For any periodic array, defined by (B1), which $\forall\mathbf{R}_p=(R_p,\varphi_p)$ also contains the vector $-\mathbf{R}_p=(R_p,\varphi_p+\pi)$, the lattice sums (B12) satisfy the relation

$$\sigma_n = (-1)^n\sigma_n. \tag{B13}$$

Therefore, in this case, only the lattice sums of even order appear in (B11). The sum σ_2 is conditionally convergent and depends on the direction of the applied field [4,5,11,12,14]. Therefore, we will denote it by $\sigma_2(\gamma)$. The sums of order $n\geq 3$ are absolutely convergent.

Then by means of the binomial expansion

$$\begin{aligned}\zeta^n &= c^n(\cosh w-\cosh w_0)^n\\ &= \left(\frac{c}{2}\right)^n\sum_{k,\ell=0}^{n}\binom{n}{k}\binom{n}{\ell}(-1)^{k+\ell}e^{(k+\ell-n)w}e^{(k-\ell)w_0},\end{aligned} \tag{B14}$$

we may recast the Green's function (B3) in the form

$$\begin{aligned}G(\mu,\theta;\mu_0,\theta_0) = &-\ln\frac{c}{2} - \mu\\ &+ 2\sum_{n=1}^{\infty}\frac{e^{-n\mu}}{n}[\cosh(n\mu_0)\cos(n\theta_0)\cos(n\theta)\\ &+ \sinh(n\mu_0)\sin(n\theta_0)\sin(n\theta)]\\ &+ \mathrm{Re}\left\{\sum_{n=1}^{\infty}\left(\frac{c}{2}\right)^n\frac{\sigma_n}{n}\left[\sum_{k,\ell=0}^{n}\binom{n}{k}\binom{n}{\ell}\right.\right.\\ &\left.\left.\times(-1)^{k+\ell}e^{(k+\ell-n)w}e^{(k-\ell)w_0}\right]\right\}.\end{aligned} \tag{B15}$$

Note that this series expansion of the Green's function is valid only inside the unit cell, where $|\mathbf{r}-\mathbf{r}_0|<R_p$, $\forall p\neq 0$, and for $\mu>\mu_0$. Hence, if μ_0 defines the ellipse (C), then the series expansion (B15) is valid in the region between the ellipse (C) and the boundary of the unit cell (see Fig. 1). The Green's function (83) is unique to within a constant so that, we can remove from (B15) the constant term $\ln(c/2)$.

If the array has the property that $\forall\mathbf{R}_p=(R_p,\varphi_p)$ it also contains the vector $\mathbf{R}'_p=(R_p,-\varphi_p)$, then the lattice sums are real. An example of such an array is the rectangular array with the fundamental translation vectors $\hat{\mathbf{e}}_1=(a,0)$ and

$\hat{\mathbf{e}}_2=(0,b)$, where a and b are the sides of the unit cell. Thus the representation in the complex plane of the array vectors (B1) has the form

$$z_p=p_1a+ip_2b, \quad p=(p_1,p_2)\in\mathbb{Z}^2. \tag{B16}$$

Note that when $a>b$ the condition (B9) becomes

$$|\zeta|<\min(|z_p|)=b. \tag{B17}$$

Also, the Green's function (B15) takes the form

$$\begin{aligned}G(\mu,\theta;\mu_0,\theta_0)=&-\mu\\&+2\sum_{n=1}^{\infty}\frac{e^{-n\mu}}{n}[\cosh(n\mu_0)\cos(n\theta_0)\cos(n\theta)\\&+\sinh(n\mu_0)\sin(n\theta_0)\sin(n\theta)]\\&+\sum_{n=1}^{\infty}\left(\frac{c}{2}\right)^{2n}\frac{\sigma_{2n}}{2n}\sum_{k,\ell=0}^{2n}\binom{2n}{k}\binom{2n}{\ell}\\&\times(-1)^{k+\ell}e^{(k+\ell-2n)\mu}e^{(k-\ell)\mu_0}\{\cos[(k\\&+\ell-2n)\theta]\cos[(k-\ell)\theta]-\sin[(k+\ell\\&-2n)\theta]\sin[(k-\ell)\theta]\}.\end{aligned} \tag{B18}$$

The Green's function (B18) is doubly periodic and fully factorized in the variables μ, θ, μ_0, and θ_0.

APPENDIX C: THE GREEN'S THEOREM

In (5) the potential V_e is the general solution of the Laplace equation and the Green's function G satisfies (B2). Hence we have

$$\begin{aligned}V_e(\mu,\theta)=&\frac{1}{2\pi}\oint_{\partial U}\left(G\frac{\partial V_e}{\partial n'}-V_e\frac{\partial G}{\partial n'}\right)d\ell'\\&+\frac{1}{2\pi}\oint_{\partial C}\left(G\frac{\partial V}{\partial n_0}-V\frac{\partial G}{\partial n_0}\right)d\ell_0.\end{aligned} \tag{C1}$$

Here to simplify the formulas we have omitted the arguments of V_e and G in integrals. Also, the integration variables in the second integral correspond to the ellipse (C). By means of the periodicity properties of V_e and G we find that the first integral in (C1), along the boundary of the unit cell, gives the potential of the applied field

$$V_0(\mu,\theta)=E_0c(\cosh\mu\cos\theta\cos\gamma+\sinh\mu\sin\theta\sin\gamma). \tag{C2}$$

In the second integral, we change the direction of the normal, exterior to the ellipse, and use the element of arc length along the ellipse [22]

$$d\ell_0=h_{\mu_0}d\theta_0, \quad h_{\mu_0}=c\sqrt{\sinh^2\mu_0+\sin^2\theta_0}. \tag{C3}$$

The normal derivative on the ellipse has the form $\partial/\partial n_0=(1/h_{\mu_0})\partial/\partial\mu_0$, so that (C1) takes the form

$$V_e(\mu,\theta)=V_0(\mu,\theta)-\frac{1}{2\pi}\int_0^{2\pi}\left(G\frac{\partial V_e}{\partial\mu_0}-V_e\frac{\partial G}{\partial\mu_0}\right)d\theta_0. \tag{C4}$$

By substituting (3) for V_e and (B18) for the Green's function, in the integral in (C4) we have

$$\begin{aligned}&\frac{1}{2\pi}\int_0^{2\pi}\left(G\frac{\partial V_e}{\partial\mu_0}-V_e\frac{\partial G}{\partial\mu_0}\right)d\theta_0\\&=-\sum_{n\,\mathrm{odd}}[B_n^e\cos(n\theta)+B_n^o\sin(n\theta)]\left(\frac{2}{c}\right)^n e^{-n\mu}\\&\quad+\sum_{m\,\mathrm{odd}}\sum_{n=m}^{\infty}\sum_{\ell=0}^{2n-m}\left\{\left(\frac{c}{2}\right)^{2n-m}\binom{2n}{\ell+m}\binom{2n}{\ell}\frac{m}{2n}\sigma_{2n}\right.\\&\quad\times[B_m^e\cos(2\ell+m-2n)\theta\\&\quad\left.-B_m^o\sin(2\ell+m-2n)\theta]e^{(2\ell+m-2n)\mu}\right\}.\end{aligned} \tag{C5}$$

With (3) and (C5) substituted in (C4) we obtain (6).

[1] G. B. Smith, Opt. Commun. **71**, 279 (1989).
[2] G. B. Smith, Appl. Opt. **29**, 3685 (1990).
[3] A. Lakhtakia and R. Messier, Opt. Eng. **33**, 2529 (1994).
[4] Lord Rayleigh, Philos. Mag. **34**, 481 (1892).
[5] W. T. Perrins, D. R. McKenzie, and R. C. McPhedran, Proc. R. Soc. London A **369**, 207 (1979).
[6] R. C. McPhedran and D. R. McKenzie, Appl. Phys. **23**, 223 (1980).
[7] W. T. Perrins, M. Sc. thesis, The University of Sydney, Australia, 1981.
[8] I. Runge, Z. Tech. Phys. **6**, 61 (1925).
[9] N. A. Nicorovici, R. C. McPhedran, and G. W. Milton, Proc. R. Soc. London A **442**, 599 (1993).
[10] N. A. Nicorovici, D. R. McKenzie, and R. C. McPhedran, Opt. Commun. **117**, 151 (1995).
[11] R. C. McPhedran and D. R. McKenzie, Proc. R. Soc. London A **359**, 45 (1978).
[12] D. R. McKenzie, R. C. McPhedran, and G. H. Derrick, Proc. R. Soc. London A **362**, 211 (1978).
[13] R. C. McPhedran and A. B. Movchan, J. Mech. Phys. Solids **42**, 711 (1994).
[14] A. B. Movchan, N. A. Nicorovici, and R. C. McPhedran, Proc. R. Soc. London A (to be published).
[15] G. K. Batchelor, Annu. Rev. Fluid Mech. **6**, 227 (1974).
[16] C. L. Berman and L. Greengard, J. Math. Phys. **35**, 6036 (1994).
[17] J. Helsing, J. Mech. Phys. Solids **42**, 1123 (1994).
[18] F. L. Galeener, Phys. Rev. Lett. **27**, 421 (1971); **27**, 769 (1971); **27**, 1716 (1971).
[19] R. Landauer, *Electrical Conductivity in Inhomogeneous Media*, in *Electrical Transport and Optical Properties of Inhomogeneous Media*, edited by J. C. Garland and D. B. Tanner (AIP, New York, 1978).
[20] R. W. Cohen *et al.*, Phys. Rev. B **8**, 3689 (1973).

[21] P. M. Morse and H. Feshbach, *Methods of Theoretical Physics* (McGraw-Hill, New York, 1953).
[22] J. Meixner and F. W. Schäfke, *Mathieusche Funktionen und Sphäroidfunktionen* (Springer-Verlag, Berlin, 1954).
[23] J. A. Osborn, Phys. Rev. **67**, 351 (1945).
[24] C. J. F. Böttcher, *Theory of Electric Polarization* (Elsevier, Amsterdam, 1973).
[25] W. K. H. Panofsky and M. Phillips, *Classical Electricity and Magnetism*, 2nd ed. (Addison-Wesley, Reading, MA, 1962).
[26] B. W. Ninham and R. A. Sammut, J. Theor. Biol. **56**, 125 (1976).
[27] G. K. Batchelor and R. W. O'Brien, Proc. R. Soc. London A **355**, 313 (1977).
[28] W. H. Press *et al.*, *Numerical Recipes in FORTRAN*, 2nd ed. (Cambridge University Press, New York, 1994).
[29] Shih-Yuan Lu, J. Appl. Phys. **76**, 2641 (1994).
[30] J. Nevard and J. B. Keller, J. Math. Phys. **26**, 2761 (1985).